buildings

Article

Probabilistic Assessment of Buildings Subjected to Multi-Level Earthquake Loading Based on the PBSD Concept

J. Guadalupe Monjardin-Quevedo [1], Federico Valenzuela-Beltran [2], Alfredo Reyes-Salazar [2], J. Martin Leal-Graciano [2], Xochitl G. Torres-Carrillo [1] and J. Ramon Gaxiola-Camacho [2,*]

1 Department of Earth and Space Sciences, Autonomous University of Sinaloa, Culiacán 80013, Mexico
2 Department of Civil Engineering, Autonomous University of Sinaloa, Culiacán 80013, Mexico
* Correspondence: jrgaxiola@uas.edu.mx

Abstract: An alternative probabilistic assessment of buildings excited by multi-level seismic loading is presented in this paper. This evaluation is developed for both steel and reinforced concrete buildings using the Performance-Based Seismic Design (PBSD) concept. The methodology implements Probability Density Functions (PDFs) of inter-story drifts to extract structural risk in terms of the reliability index. Ten buildings of steel and reinforced concrete, respectively, are designed considering different locations in Mexico. Then, each structure is excited by ground motions representing different earthquake intensity levels for three performance levels: immediate occupancy, life safety, and collapse prevention. The deterministic seismic response of buildings is extracted using the finite element software OpenSees. Based on the results, it can be stated that the probabilistic assessment technique represents an efficient approach for extracting the seismic risk of structures using PDFs of inter-story drifts. Lastly, it is demonstrated that the evaluation of buildings following PBSD is a step in the right direction, moving from traditional deterministic design concepts to probabilistic philosophies.

Keywords: performance-based seismic design; probability density functions; reliability index; structural risk; ground motion selection; performance levels; earthquake-resistant design

check for updates

Citation: Monjardin-Quevedo, J.G.; Valenzuela-Beltran, F.; Reyes-Salazar, A.; Leal-Graciano, J.M.; Torres-Carrillo, X.G.; Gaxiola-Camacho, J.R. Probabilistic Assessment of Buildings Subjected to Multi-Level Earthquake Loading Based on the PBSD Concept. *Buildings* **2022**, *12*, 1942. https://doi.org/10.3390/buildings12111942

Academic Editor: Humberto Varum

Received: 22 September 2022
Accepted: 8 November 2022
Published: 10 November 2022

1. Introduction

The Performance-Based Seismic Design (PBSD) philosophy can be considered a new concept for designing seismic-resilient buildings subjected to multi-level earthquake loading. In general, the main objective of PBSD is to control structural damage provoked by ground motions of different characteristics that may impact buildings. Such a novel design paradigm represents an alternative to the traditional deterministic design concept that is used on a daily basis by structural engineers [1,2]. In this sense, it is well-known that the fundamental goal of earlier building codes, which were used based on a force-based design, was to consider one performance level depending on the importance of the building type. In other words, the main objective was based on avoiding structural collapse under the maximum considered earthquake that may occur in the building location. However, although several sections of modern seismic codes address limiting structural damage by capacity design, in most of the guidelines very little is recommended to guarantee that the structural performance caused by seismic loading will be within safety limits. Some weaknesses of several codes, in terms of controlling structural damage, have been exhibited due to the impact of several ground motions around the world. For example, the 1985 Mexico City earthquake caused around 4 billion USD in terms of structural damage [3]. At the end of October 1989, in the region of Loma Prieta, California, a 6.9 Mw magnitude earthquake was recorded, causing structural damage of around 6 billion USD [4]. Some years later, in January 1994, a 6.7 Mw magnitude earthquake resulted in structural damage of around 30 billion USD [5]. One year later in 1995, the 6.9 Mw earthquake in Kobe, Japan, left economic losses of around 150 billion USD [6]. Therefore, the above-documented ground motions caused exorbitant structural damage. This was a situation of special concern for structural engineers since traditional building codes of that time only guaranteed safe structural conditions for one performance objective. As a result, the structural engineering community realized that some other performance levels had to be explored to reduce structural damage.

Based on the facts reported above, several research projects were funded in the late 1990s. The studies were mainly developed in the United States and represented the beginning of a new design paradigm generally known as PBSD [7–10]. Among some of the most important results documented in these projects, was the necessity to develop alternative methodologies for extracting the structural reliability of buildings subjected to multi-level ground motions. Thus, calculation of the structural reliability of buildings excited by seismic loading was highlighted as important in implementing PBSD. In this context, some of the most common approaches to extracting the seismic risk of structures are very advanced. However, they may not be suitable for use in the PBSD philosophy. For example, the Pacific Earthquake Engineering Research center established a reliability method known as direct differentiation method [11–13]. However, they assumed mean values of structural parameters and the loading was not applied in the time domain for the structures under consideration. In summary, they implemented an out-crossing approach [14] using an importance sampling scheme [15,16]. Au & Beck (1999) [17] implemented an adaptive importance sampling approach to extract multidimensional integrals generally present in reliability analysis. Unfortunately, multidimensional integrals are implicit for nonlinear structural problems. Other scholars [18–20] studied the seismic performance of structures. In this research, they documented the need for reliability-based PBSD approaches. Wen (2001) [21] introduced a reliability-based framework to be implemented according to the PBSD philosophy. However, a physics-based analytical methodology for the structural analysis was not applied.

For the case of PBSD of reinforced concrete structures, the following studies have been recently reported in the literature. Liao & Goel (2014) [22] presented the first-time application of PBSD by considering the plasticity of reinforced concrete special moment frames. They implemented pre-established target drift and yield mechanisms as the performance objectives of four reinforced concrete buildings. In the end, it was demonstrated with the help of pushover and response history analyses that the seismic responses of the buildings met the targeted performance criteria, which improved the corresponding baseline of buildings designed with the code. A few years later, a study was published on the PBSD of reinforced concrete structures based on an improved risk-targeted design objective (Franchin et al., 2018) [23]. In summary, the performance objectives were formulated in terms of maximum accepted mean annual frequency of exceedance while considering multiple limit states. The approach was implemented on a 15-story plane frame building. Their results demonstrated that the approach was very applicable for the PBSD of reinforced concrete structures with explicit targets in terms of anticipated levels of risk (Franchin et al., 2018) [23]. On the other hand, for steel structures, several technical publications and reports can be found in the literature. For instance, Harris & Speicher (2018) [24] documented an investigation into the seismic performance of steel special moment frames considering the recommendations of the ASCE 41-13 (2014) [25] guidelines. They found that steel special moment frames designed using the traditional building code (ASCE 7-16, 2016) [26] struggle to meet the acceptance criteria of ASCE 41-13 (2014) [25]. In other words, the steel special moment frames did not satisfy diverse performance levels evaluated with respect to the ASCE 41-13 (2014) [25] guidelines. In some investigations, the PBSD concept has been successfully implemented with the help of reliability analysis considering seismic loading in the time domain and various sources of non-linearities as well as uncertainties [27–29]. In addition, some other scholars have documented the PBSD of moment resisting steel frames using an adaptive optimization framework and optimum design load patterns (Moghaddam et al., 2021) [30]. In summary, a performance-based optimization process was developed for determining the optimal cross-sectional distribution of steel moment resisting frames subjected to seismic loading. Based on the results, it was reported that the proposed method was very efficient in improving the seismic performance of the designed structures. Furthermore, the analyzed buildings presented up to 70% less global damage compared with the similar frames that were designed based on traditional code load patterns. Very recently, Monjardin-Quevedo et al. (2022) [31] presented an investigation about the seismic risk of steel special moment frames with deep columns considering the PBSD concept. In summary, they found that the use of deep columns in steel special moment frames is a step in the right direction to reducing the lateral displacement and cost of steel structures subjected to seismic loading.

Undoubtedly, the above studies represent important progress in the state-of-the-art of PBSD reliability techniques for reinforced concrete and steel buildings. However, there are several knowledge gaps that must be filled. For example, to evaluate the variability in earthquake hazards, multi-level ground motions must be used to explicitly extract the reliability of buildings. In addition, if the seismic vulnerability of structures in a particular country needs to be studied, multiple locations must be evaluated. Furthermore, seismic loading is an extremely random variable. It is reported in the literature that selection of ground motion records for nonlinear response history analysis is a critical step since it considerably affects the performance of the buildings under consideration (Demir, 2022) [32]. Furthermore, it has been documented that if the number of ground motion records in a particular suite of them is lower than seven, very conservative seismic structural responses will be extracted since the maximum rather than mean response values will be considered (Demir, 2022) [32]. Thus, there is a necessity to assess its random behavior. These are only a few of the problems that must be addressed to properly implement the PBSD concept. As an alternative solution to these issues, in this paper, a novel approach based on the PBSD philosophy is presented which involves probabilistic assessments of buildings subjected to multi-level earthquake loadings. Several locations in Mexico are evaluated, and both reinforced concrete and steel buildings are considered. In summary, inter-story drifts of steel and reinforced concrete structures are computed using OpenSees (Open System for Earthquake Engineering Simulation) finite element software (Mazzoni et al., 2006) [33]. Then, PDFs of inter-story drifts are constructed and evaluated to calculate the seismic risk in terms of the reliability index (β).

2. Probabilistic Assessment Approach to Extract Structural Risk

Numerous studies investigating the suitable calculation of structural risk of buildings subjected to ground motions have been conducted by many authors; however, this problem is still insufficiently explored, and several aspects remain to be addressed. In this regard, the present paper introduces a novel probabilistic assessment approach to extract structural risk, which may be an ideal tool to properly implement the PBSD concept.

2.1. Deterministic Response Using OpenSees

One of the most important parts of the probabilistic assessment approach presented in this paper is the calculation of the deterministic response of buildings subjected to earthquakes. In this paper, for both steel and reinforced concrete buildings, the deterministic response under the action of multi-level earthquake loading is extracted with the help of OpenSees software (Mazzoni et al., 2006) [33]. It is also worth mentioning that to obtain valuable information about structural performance, nonlinear time history analyses were performed to extract the response of the buildings considering each of the selected ground motions. In addition, for the models used in the OpenSees finite element software, the following items were considered: beam-column elements, bilinear hysteretic models with degradation, and time-dependent dynamic loads considering earthquake acceleration input at all nodes restrained in specified direction.

2.2. Seismic Load Selection and Performance Levels

The selection of seismic load is a very important step in the process of the probabilistic approach to be implemented in this research. In this context, it is demonstrated that the selection of suitable ground motion records for nonlinear dynamic analysis is critical since it significantly impacts the structural responses which are used for seismic performance assessment of buildings (Demir et al., 2021) [34]. The ground motion selection strategy used in this paper is summarized as follows. First the structural models (buildings) must be designed to extract their fundamental vibration period. Then, a target response spectrum is generated depending on the location of the building. This represents the seismic hazard of the region. Afterwards, a database of real records of ground motions is used to scale the response spectrum of every earthquake, selecting those with a scale factor as near as possible to one. In addition, it is important to mention that following the PBSD concept, three performance levels must be considered in the selection of seismic load: Immediate Occupancy (IO), Life Safety (LS), and Collapse Prevention (CP). These performance levels are related to return periods of 72, 475, and 2475 years, respectively. Furthermore, eleven ground motions are selected for every performance level. Thus, for the reliability analysis of one building based on the PBSD concept, thirty-three ground motions must be selected that represent all the recommended performance levels. This part of the approach will be clarified later in this paper with the help of the numerical examples.

2.3. Probability Density Functions (PDFs) of Inter-Story Drifts

As previously mentioned, the structural response to be used by the probabilistic approach developed in this research is the inter-story drift of steel and reinforced concrete buildings. It is important to mention that in the probabilistic assessment, PDFs are generated for every inter-story drift considering several distributions. Then, considering the generated PDFs for every inter-story drift, a Chi-squared test is performed to select the best-fit PDF of the inter-story drift, and the PDF is used for the calculation of the reliability index as discussed in the following section.

2.4. Calculation of Reliability Index

For the computation of the reliability index, the concept of probability of failure (p_f) and probability of survival (p_s) must be introduced. In this context, p_f and p_s refer to unsafe and safe condition of the building or structure under consideration, respectively. Hence, in the design process, the p_f must be maintained as low as possible. On the other hand, the p_s can be evaluated as simply $1 - p_f$. In other words, p_s is the complement of p_f. This is illustrated in Figure 1. There are several steps involved in the construction of the PDF illustrated in Figure 1. First, the probabilistic assessment approach extracts the structural response coming from the nonlinear time history analysis of every considered ground motion in terms of inter-story drift. Then, the inter-story drifts are arranged in increasing order, and a subdivision of the collected data is performed. Subsequently, equal intervals are formed and the observations in each interval are counted. Afterwards, the number of observations in every interval versus inter-story drift are plotted to form a histogram illustrating the randomness of inter-story drift. To extract information about the probability of events of interest, the area under the histogram is converted to 1.0, and the histogram of inter-story drift is then transformed to a frequency diagram. Thus, the frequency diagram is the basis for selection of the best-fit PDF of inter-story drift. This is found using a Chi-squared goodness of fit test that demonstrates the confidence of the selected PDF that is represented, as shown in Figure 1.

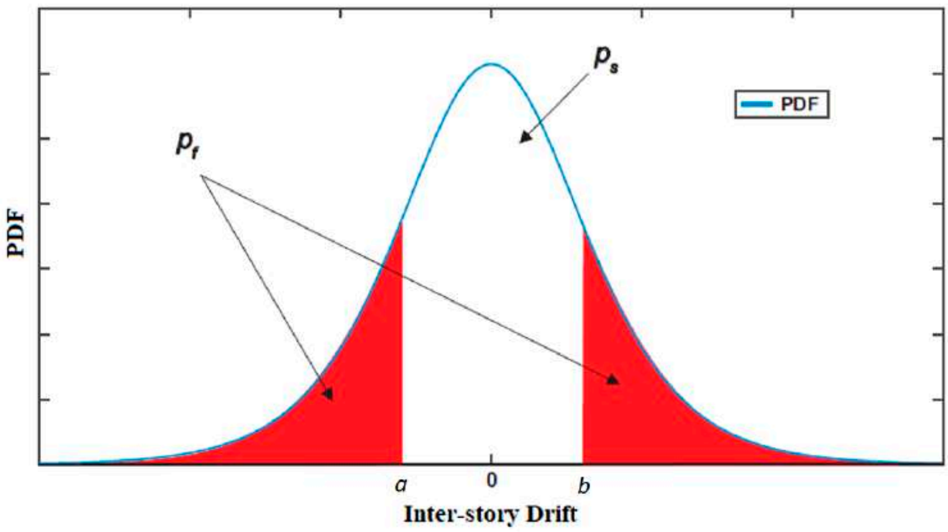

Figure 1. PDF of inter-story drift with limits a and b.

Considering a and b as the limits that establish the boundaries of safety and failure (see Figure 1), then p_f can be estimated as follows (Nowak & Collins, 2012) [35]:

$$p_f = 1 - P(a < X \leq b) \tag{1}$$

where X represents the inter-story drift responses from the evaluated structural model; and a and b are certain limits defining the level of security of the building. In this paper, the limits a and b are ± 0.007, ± 0.025, and ± 0.050 for IO, LS, and CP performance levels, respectively.

Focusing on the right-hand side of Equation (1), the value of $P(a < X \leq b)$ can be extracted as (Nowak & Collins, 2012) [35]:

$$P(a < X \leq b) = \int_a^b f_x(x)dx \tag{2}$$

where $f_x(x)$ is the best-fit PDF of inter-story drift based on the Chi-squared test of the following eleven distributions: (1) normal, (2) lognormal, (3) Birnbaun–Saunders, (4) extreme value (EV), (5) gamma, (6) generalized extreme value (GEV), (7) logistic, (8) loglogistic, (9) stable, (10) t location scale (tLS), and (11) Weibull (Vazquez-Ontiveros et al., 2021) [36]. It must be stated that more distributions can be used to represent PDFs of inter-story drift; however, in this research only the above-mentioned eleven distributions are used.

In general, buildings are constantly interacting with several demands including live and dead loads, seismic and wind loading, etc. These may cause certain structural deterioration. Thus, it is very important to explicitly know the reliability of buildings in terms of a specific factor. Such a factor or index is commonly known in the literature as the reliability index (Nowak & Collins, 2012) [35]. Most of the time, the reliability index (β) is the safety associated with a system to achieve the required function under specific performance conditions during a given period (Lemaire, 2013) [37]. In this context, β is related to p_f as follows:

$$\beta = \Phi^{-1}\left(1 - P_f\right) \tag{3}$$

where Φ^{-1} is the inverse of the Cumulative Distribution Function (CDF) that is related to the best-fit PDF of inter-story drift.

2.5. Flowchart of the Probabilistic Approach

A summary of the process behind the alternative probabilistic approach presented in this paper is shown in Figure 2. This flowchart can be reviewed as follows. First, the structural models are selected. In the case of this paper, two building types (steel and reinforced concrete) are studied which are located strategically at ten different locations in Mexico. Then, performance levels are selected. In this research, IO, LS, and CP are used for the evaluation. The seismic loading selection is then developed for the first period of vibration of the structure under consideration, and a target response spectrum of the location under consideration. Once the seismic loading is carefully chosen, nonlinear time history analyses are performed in OpenSees software, considering each ground motion to extract the seismic performance of the structure in terms of inter-story drift. Next, eleven PDFs are constructed for each of the nonlinear response of the buildings to represent the randomness of inter-story drift. This is quite important because from among these PDFs, one is selected representing the best-fit PDF of inter-story drift, which is used for the calculation of p_f and β, respectively.

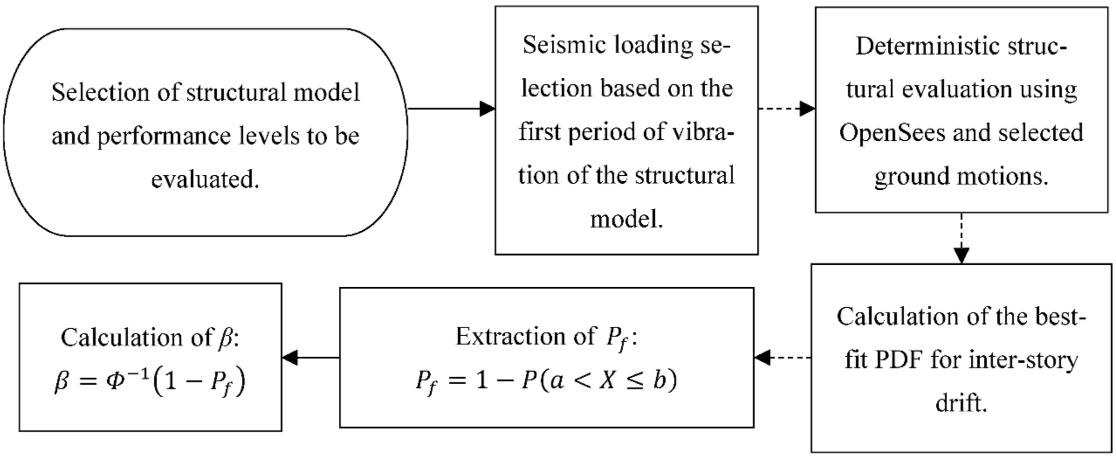

Figure 2. Flowchart of the alternative probabilistic approach.

3. Numerical Examples for the Implementation of the Probabilistic Approach

In this part of the paper, ten buildings of reinforced concrete and steel, respectively, are used to implement the probabilistic approach. These structures are designed based on Mexico's building code (MCBC, 2017) [1] for ten different locations of the country. In addition, the PBSD concept is considered in the seismic risk evaluation based on three performance levels: IO, LS, and CP.

3.1. Structural Models and Locations

The structural configurations of the ten buildings of reinforced concrete and steel are illustrated in Figure 3, and period of vibration of every building is summarized in Table 1.

In Figure 3, it can be observed that there are structural configurations with bay widths of 9 m in both horizontal directions. These dimensions are used because such structures are office buildings with wide spaces. This is something that nowadays is becoming very popular in Mexico.

The ten locations of the above-mentioned buildings were selected based on the four seismic zones that the building code of Mexico stipulates as A, B, C, and D, respectively (MCBC, 2017) [1]. Seismic zone A is the lowest earthquake-prone region of the country. Seismic zone B represents a region with moderate ground motion hazard. Zone C presents a high seismic risk, and finally, zone D represents the region in Mexico where the most severe earthquakes may occur. Based on the above facts, ten locations were selected covering the four seismic zones of Mexico. Table 2 summarizes the exact location of the buildings and the corresponding seismic zone considered in this research. In addition, Table 2 illustrates the precise position of every building over the map of Mexico. It is observed in Table 2 that the ten selected cities for this research are well-distributed around the country.

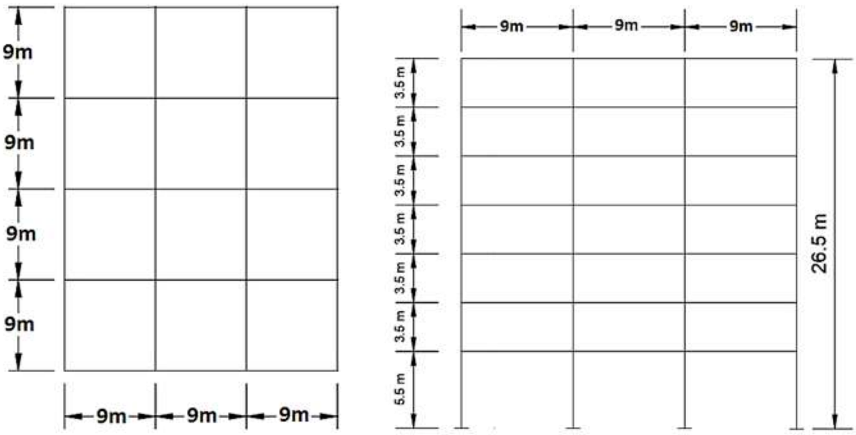

(**a**) (**b**)

Figure 3. (**a**) Plan, (**b**) Elevation. Structural configurations of the reinforced concrete and steel buildings.

Table 1. Period of vibration of buildings.

City	Reinforced Concrete (s)	Steel (s)
Agua Prieta, Sonora	1.6828	1.196
Cd. Victoria, Tamaulipas	1.8024	1.162
Culiacan, Sinaloa	1.8024	1.2846
Mexicali, Baja California	0.8416	1.1115
Torreon, Coahuila	1.8024	1.1929
Chilpancingo, Guerrero	0.9057	1.2950
Guadalajara, Jalisco	1.5675	1.3042
Mérida, Yucatan	1.8024	1.3042
Oaxaca de Juarez, Oaxaca	1.2745	1.2772
Villahermosa, Tabasco	1.6136	1.3042

Table 2. Location and corresponding seismic zone of buildings.

City	Seismic Zone	Location on Map
Agua Prieta, Sonora	C	
Ciudad Victoria, Tamaulipas	A	
Culiacan, Sinaloa	B	
Mexicali, Baja California	D	
Torreon, Coahuila	A	
Chilpancingo, Guerrero	D	
Guadalajara, Jalisco	C	
Merida, Yucatan	A	
Oaxaca de Juarez, Oaxaca	D	
Villahermosa, Tabasco	B	

In summary, for each of the ten cities presented in Table 2, two buildings were designed (reinforced concrete and steel, respectively) following the building code of Mexico (MCBC, 2017) [1]. Thus, in total, twenty buildings are studied in this research and their corresponding reliability index is extracted considering the three performance levels mentioned earlier.

3.2. Selection of Representative Ground Motions

In the case of Mexico, if 3D time history nonlinear analyses are implemented, the building code recommends the selection of at least seven pairs of ground motion records as representatives of the location's corresponding seismic hazard in the zone (MCBC, 2017) [1]. On the other hand, if 2D response history analyses are used, the code recommends the use of at least seven representative ground motion records. For this paper, 2D time history analyses were utilized; hence, eleven ground motions are selected, which clearly satisfies the requirements of the building code (MCBC, 2017) [1]. As mentioned in Section 2.2, the selection of representative ground motions considers two technical items: (1) the spectral shape of target response spectrum, which depends on the seismic zone; and (2) the matching of ground motion spectral acceleration to the target response spectrum at the first period of vibration of the building, applying a scale factor to all the domain of ground motion spectrum. In summary, the selected ground motions are those that have a similar spectral shape to the target spectrum and are anchored at the first mode of vibration of the building using scale factors close to one. It is also important to mention that the target response spectrum for every site is generated considering the probability of the exceedance and return period of each performance level summarized in Table 3 (SEAOC Vision 2000, 1995) [7].

Table 3. Selection of ground motions based on performance levels.

Selected Ground Motions		
Probability of Exceedance	**Return Period (Years)**	**Performance Level**
50% in 50 years	72	IO
10% in 50 years	475	LS
2% in 50 years	2475	CP

In this context, some of the most common building codes recommend the use of at least eleven representative ground motions of the zone under consideration to perform non-linear dynamic analysis of structures (ASCE 7-16, 2016; IBC, 2012) [2,26]. Thus, since three performance levels are considered in this research, eleven representative ground motions are selected considering each of the performance levels under study. Hence, for every location studied in this paper, thirty-three ground motions are selected for both the reinforced concrete and steel buildings, resulting in a total of sixty-six ground motions selected per city. The process behind the ground motion selection is shown in Figure 4.

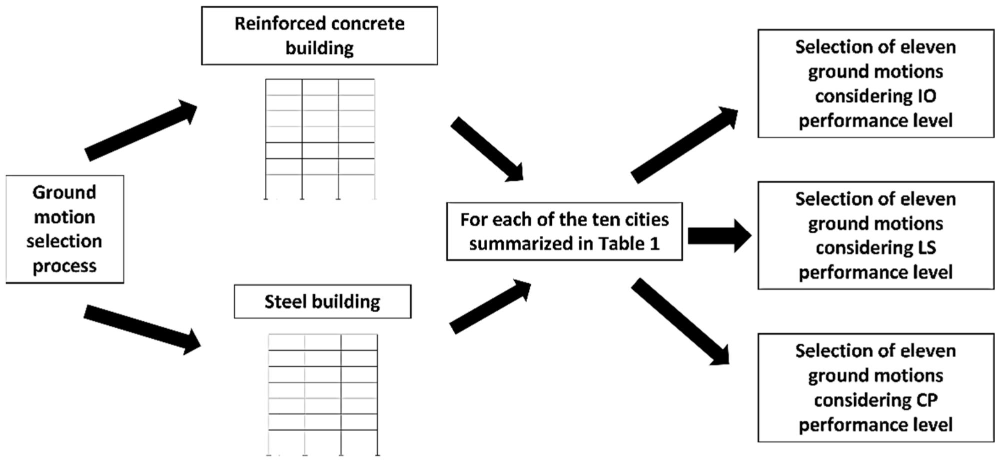

Figure 4. Ground motion selection process.

It must be also stated that the representative ground motion records of the zone are selected from a database with more than 20,000 records. Such a database is open to public access, and was generated by the Institute of Engineering at the National Autonomous University of Mexico. For the sake of illustration, Figures 5–7 present the ground motions selected considering return periods of 72, 475 and 2475 years for the city of Agua Prieta, Sonora, with reference to the reinforced concrete building. It can be observed in such Figures that the shape of the mean spectrum of the selected ground motions is similar to the corresponding target response spectrum. This is justified because of the minimum mean square error estimator calculated with respect to mean and target spectrum. In addition, every spectrum of the selected ground motions is matching in terms of spectral acceleration at the fundamental period of the structure. Furthermore, in Figures 5–7, and most particularly in Figure 5, it is observed that for lower periods, there is a difference between the mean and target spectrum. The main reason of this difference is the selection is based on two items: (1) the period of vibration of the structure (T_1), and (2) the shape of the target response spectrum within the range from $0.2T_1$ to $1.5T_1$. It is essential to point out that such a range of periods was implemented since no large sensitivity of the buildings under consideration is expected for response spectra at highly nonlinear phases for periods longer than $1.5T_1$. In this sense, for the building under consideration in the selection illustrated in Figures 5–7, its period of vibration is 1.6828 s. Thus, the range of the period for the selection is from 0.337 to 2.524 s. In Figures 5–7, three red vertical dashed lines are observed. The one on the left represents $0.2T_1$, the middle one T_1, and the right one $1.5T_2$. Thus, we believe that differences at lower periods are justified because those spectral values are very close to the left boundary of the selection range. In fact, it is observed in Figures 5–7 that for those periods, the spectral acceleration of ground motions is decaying; therefore, the mean spectrum is becoming further from the target one.

Relevant information about the selected ground motions illustrated in Figures 5–7 is presented in Table 4. Some of the most important information about the above-mentioned ground motions is summarized including station name, magnitude, and scale factor.

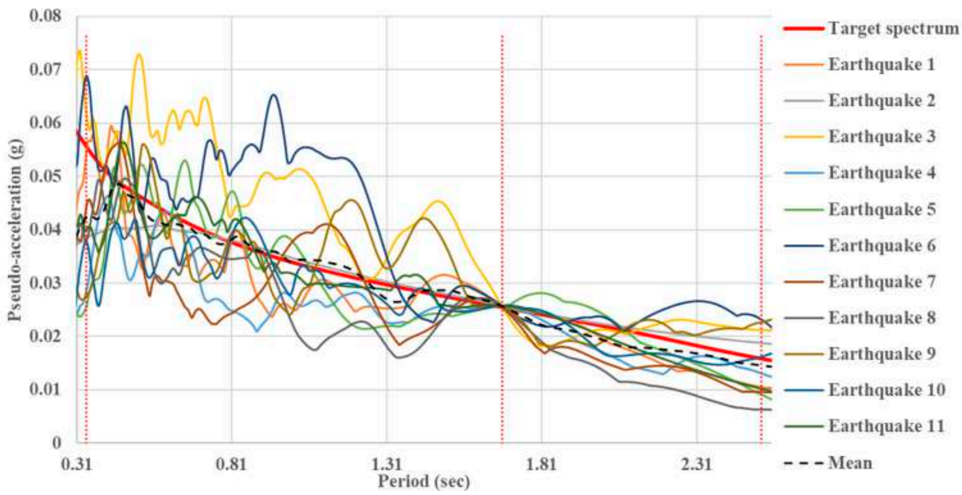

Figure 5. Ground motion selection for Agua Prieta, Sonora, corresponding to a return period of 72 years with respect to the reinforced concrete building.

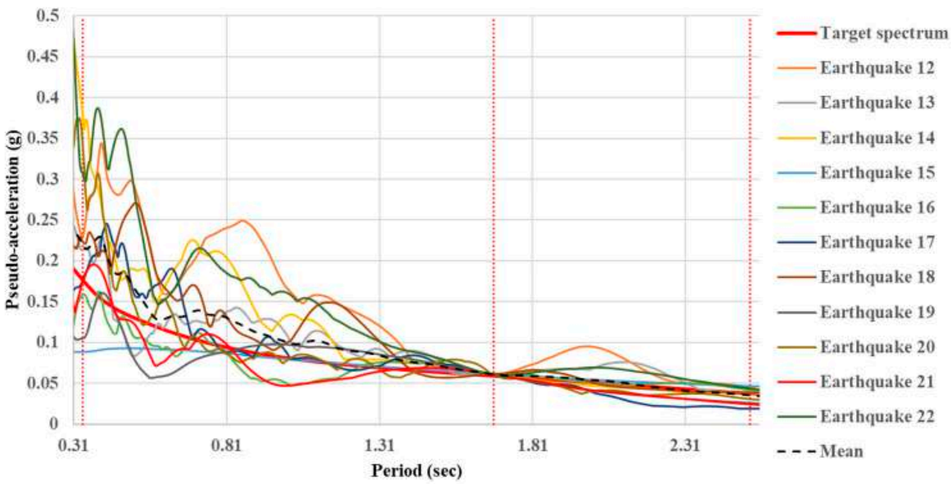

Figure 6. Ground motion selection for Agua Prieta, Sonora, corresponding to a return period of 475 years with respect to the reinforced concrete building.

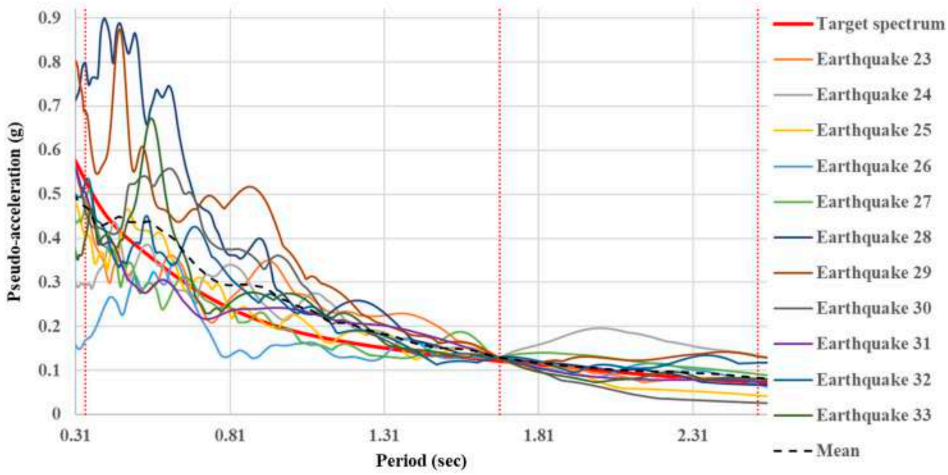

Figure 7. Ground motion selection for Agua Prieta, Sonora, corresponding to a return period of 2475 years with respect to the reinforced concrete building.

Table 4. Relevant information of selected ground motions for Agua Prieta, Sonora, corresponding to the reinforced concrete building.

Ground Motion	Performance Level	Station Name	Magnitude	Scale Factor
Earthquake 1	IO	Cerro de Piedra	4.90	0.88
Earthquake 2	IO	La Venta	6.80	0.88
Earthquake 3	IO	Mesa Vibradora	6.30	0.87
Earthquake 4	IO	Huamuxtitlan	6.4	1.0
Earthquake 5	IO	Texcoco Chimalhuacan	6.30	1.0
Earthquake 6	IO	Sismex Ciudad Universitaria	6.40	0.74
Earthquake 7	IO	Ciudad Serdan	6.5	1.5
Earthquake 8	IO	Chila de las Flores	6.5	1.1
Earthquake 9	IO	Las Mesas	6.80	0.88
Earthquake 10	IO	Sismex Hospital ABC	7.00	1.1
Earthquake 11	IO	Mezontepec	6.5	1.4
Earthquake 12	LS	Papanoa	6.80	1.3
Earthquake 13	LS	Cerro de Piedra	4.70	0.84
Earthquake 14	LS	El Ocotito	6.80	1.1
Earthquake 15	LS	Las Canteras	6.5	1.1
Earthquake 16	LS	Atoyac	6.80	1.4
Earthquake 17	LS	Apatzingan	6.10	1.9
Earthquake 18	LS	Caleta de Campos	6.20	1.6
Earthquake 19	LS	San Marcos	6.20	1.1
Earthquake 20	LS	Las Vigas	6.30	1.6
Earthquake 21	LS	San Luis de la Loma 2	6.1	0.93
Earthquake 22	LS	San Martin los Canseco	6.5	1.3
Earthquake 23	CP	Las Negras	6.5	0.94
Earthquake 24	CP	La Union	6.80	0.96
Earthquake 25	CP	Rio Grande	6.5	1.5
Earthquake 26	CP	Caleta de Campos	6.5	0.85
Earthquake 27	CP	Aeropuerto Zihuatanejo	6.30	1.0
Earthquake 28	CP	Petatlan II	7.2	2.1
Earthquake 29	CP	Sicartsa Aceracion	7.00	1.4
Earthquake 30	CP	San Marcos	6.30	1.2
Earthquake 31	CP	Caleta de Campos	6.80	0.99
Earthquake 32	CP	Villita Margen Derecha	6.80	1.4
Earthquake 33	CP	Chilpancingo	6.30	0.72

Finally, for the sake of space, only the ground motion selection for one of the locations considering its respective concrete building is presented above. However, the same process was implemented for every one of the cities reported in Table 2 for both their reinforced concrete and steel buildings. For the study presented in this paper, 660 ground motions were selected considering all the locations and both steel and reinforced concrete buildings.

3.3. Derterministic Seismic Response of Buildings

A fundamental part of this paper is the calculation of the deterministic seismic response of the buildings under consideration. As previously mentioned, inter-story drift is extracted for each structure using three sets of eleven ground motions, each with return periods of 72, 475, and 2475 years with corresponding IO, LS, and CP performance levels, respectively. To compute such a response, the open access finite element software OpenSees was utilized (Mazzoni et al., 2006) [33]. Figures 8–11 illustrate the mean value of the maximum inter-story drift for every floor level of the buildings for each of the locations under consideration (see Table 2). In addition, in Figures 8–11, the steel and reinforced concrete buildings are represented as "S" and "RC", respectively. The main intent of Figures 8–11 is to represent the mean of the maximum inter-story drift per floor level experienced by each of the buildings located in different seismic zones of Mexico.

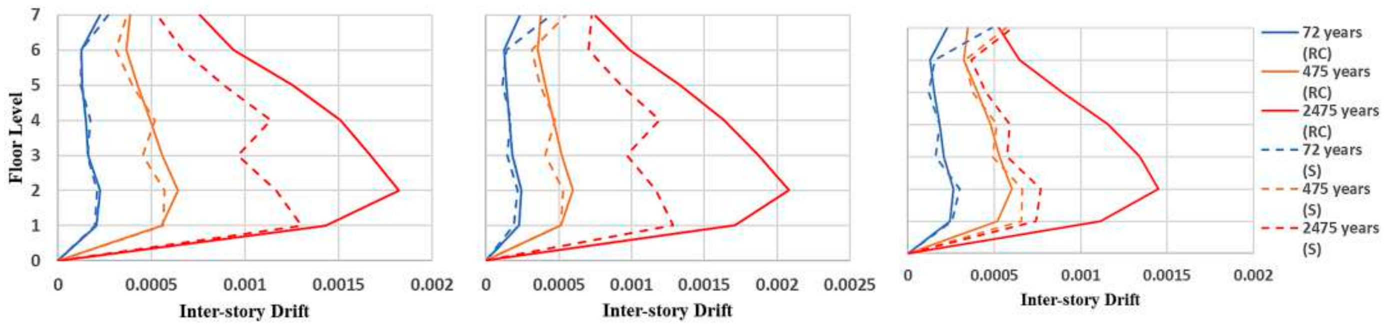

(**a**) (**b**) (**c**)

Figure 8. (**a**) Ciudad Victoria, Tamaulipas, (**b**) Ciudad Victoria, Tamaulipas, (**c**) Ciudad Victoria, Tamaulipas. Mean of the maximum inter-story drift response for each level of the steel and reinforced concrete structural model for seismic zone A.

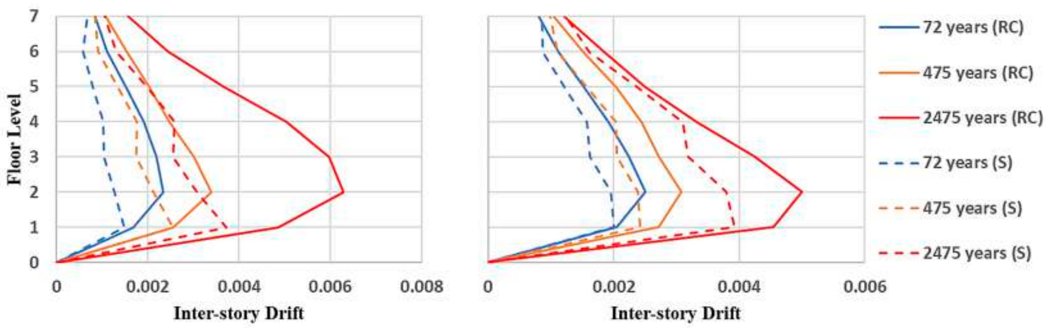

(**a**) (**b**)

Figure 9. (**a**) Culiacan, Sinaloa, (**b**) Villahermosa, Tabasco. Mean of the maximum inter-story drift response for each level of the steel and reinforced concrete structural model for seismic zone B.

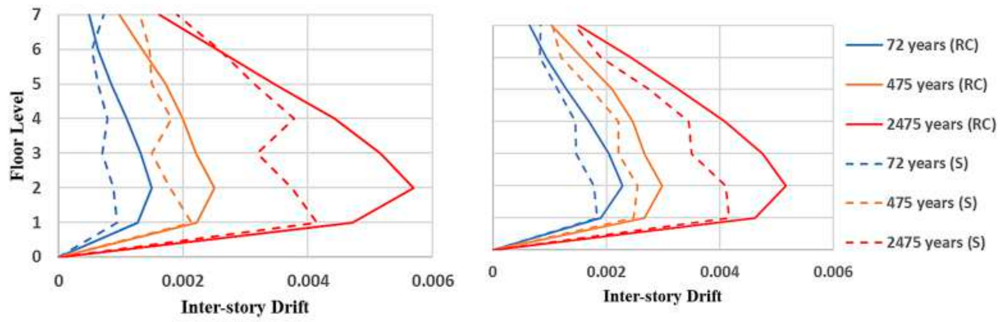

(**a**) (**b**)

Figure 10. (**a**) Agua Prieta, Sonora, (**b**) Guadalajara, Jalisco. Mean of the maximum inter-story drift response for each level of the steel and reinforced concrete structural model for seismic zone C.

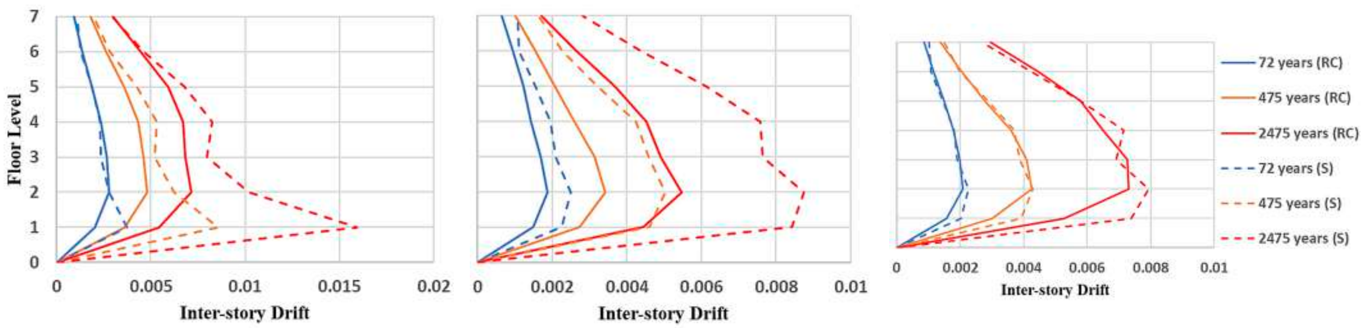

(**a**) (**b**) (**c**)

Figure 11. (**a**) Mexicali, Baja California, (**b**) Chilpancingo, Guerrero, (**c**) Oaxaca de Juarez, Oaxaca. Mean of the maximum inter-story drift response for each level of the steel and reinforced concrete structural model for seismic zone D.

Several observations can be made based on Figures 8–11. The buildings experiencing the greatest inter-story drift are those located in Chilpancingo, Mexicali, and Oaxaca de Juarez as expected, since those locations are categorized as seismic zones with the highest seismic hazard in Mexico (zone D). On the other hand, the steel and reinforced concrete buildings presenting the lowest inter-story drifts are those located in Ciudad Victoria, Torreon, and Merida. This is quite logical given that their location is classified as zone A, representing a zone with a very low seismic hazard. In terms of performance levels, for both steel and reinforced concrete buildings, the highest inter-story drifts are observed when the CP performance level is calculated for ground motions with a return period of 2475 years. In contrast, when the IO performance level is evaluated considering sets of ground motions with a return period of 72 years, the smallest inter-story drifts are observed in the buildings. This is expected because ground motions with return period of 2475 years present a greater intensity than those with return period of 72 years, which are generally earthquakes with a very low magnitude. For most of the ground motions with a return period of 2475 years in the CP performance level cases, the reinforced concrete buildings presented the greatest inter-story drifts. The floor level presenting the highest inter-story drift for almost all the cases is the second floor. This can be attributed to the fact that the height of the first floor is 5.5 m and that for all the other floors is 3.5 m. In other words, there is a change in floor heights that may produce a greater inter-story drift in the floor above. Moreover, an important observation regarding the seismic zones in Mexico (A, B, C, and D) is that for the buildings located in seismic zone A (Figure 8), the maximum inter-story drift is approximately 0.0021 for the reinforced concrete buildings and CP performance level, and the minimum inter-story drift presented is about 0.0002 for the IO performance level. It is important to mention that for buildings located in seismic zone A and evaluated with respect to IO and LS performance levels, both steel and reinforced concrete buildings presented very similar values of inter-story drift. For buildings located in seismic zone B (Figure 9), the maximum inter-story drift observed has a value close to 0.0062, and the minimum is close to 0.0009. Again, in this case, with reference to the CP performance level, the buildings presenting the greatest inter-story drift are the reinforced concrete ones. In this context, buildings located in seismic zone C (Figure 10) exhibit a very similar behavior to those located in seismic zone B with inter-story drifts ranging approximately from 0.0009 to 0.006. Within this frame of reference, buildings located in seismic zone D (Figure 11) experienced a maximum value of inter-story drift close to 0.016 and a minimum of approximately 0.002. For this case, the steel buildings present the greatest deformations in terms of inter-story drift for the CP performance level, in comparison to the seismic zones A, B, and C. Finally, it is noteworthy that buildings located in Mexicali, Baja California exhibited the largest inter-story drift, and buildings located in Merida, Yucatan presented the lowest inter-story drifts. Finally, it can be seen in Figures 8–11 that in some cases, steel buildings are more flexible than reinforced concrete buildings. However, in other cases, the behavior is the opposite. This may be caused by other factors affecting the seismic performance of buildings, such as the frequency contents of ground motions, type of soil where the structure is located, geological mechanisms of earthquakes, duration of seismic loading, resonance problems, etc. Unfortunately, incorporating these factors is beyond of the scope of this technical paper.

3.4. Structural Reliability of Buildings Using the Probabilistic Approach

Once the deterministic response is extracted for the buildings under consideration, inter-story drifts can be used to compute the structural reliability in terms of the reliability index (β) using the probabilistic approach presented in Section 2.4. To achieve this, the risk is evaluated with respect to the allowable limits summarized in Table 5. It should be noted that these limits are documented in the FEMA-350 (2000) report and their main objective is to ensure a reliable relationship of IO, LS, and CP performance levels to ground motions with return periods of 72, 475, and 2475 years, respectively.

Table 5. Permissible inter-story drift for performance level (FEMA-350, 2000).

Return Period (Years)	Performance Level	Permissible Inter-Story Drift
72	IO	$\pm$0.007
475	LS	$\pm$0.025
2475	CP	$\pm$0.050

Figures 12–21 show the results for the reliability of both steel and reinforced concrete buildings. The performance level and mean reliability index (β) are displayed in the horizontal and vertical axis, respectively. Previously introduced performance levels are evaluated (IO, LS, and CP). The mean reliability index (β) refers to the average of the reliability indexes obtained for every floor level of the building under consideration. In other words, the reliability indexes for every floor of the buildings were extracted, and then, their average for every performance level was calculated to determine the mean reliability index (β) reported in Figures 12–21. It must be also noted that possible soft-story cases may be overlooked when the mean reliability index (β) is calculated with the above procedure. However, for the buildings considered in this study, soft-story cases were not observed before calculating the mean reliability index (β).

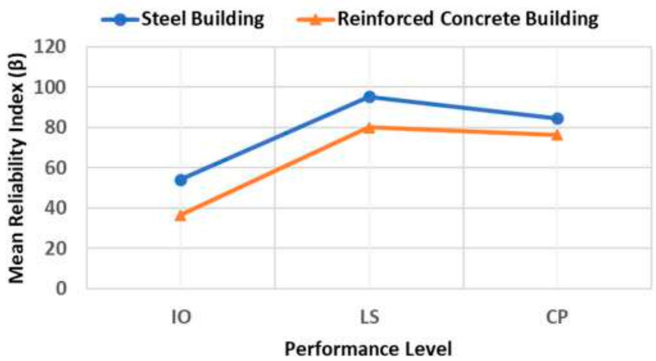

Figure 12. Mean reliability index for steel and reinforced concrete buildings located at Agua Prieta, Sonora (seismic zone C).

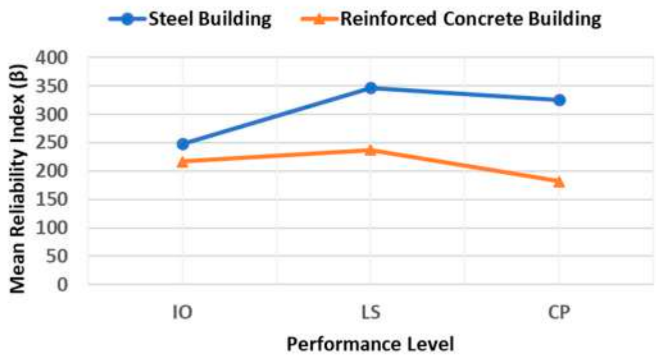

Figure 13. Mean reliability index for steel and reinforced concrete buildings located at Ciudad Victoria, Tamaulipas (seismic zone A).

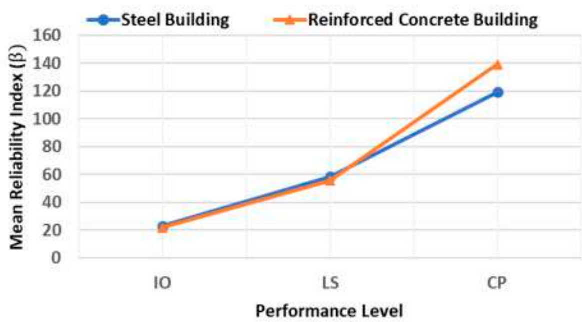

Figure 14. Mean reliability index for steel and reinforced concrete buildings located at Villahermosa, Tabasco (seismic zone B).

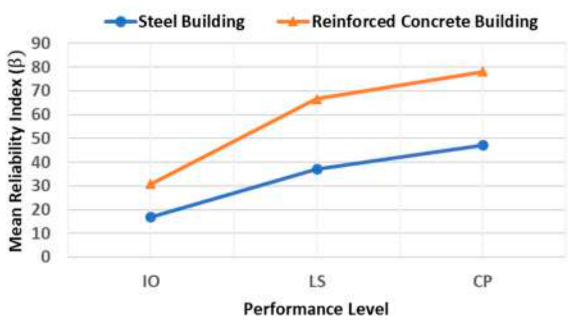

Figure 15. Mean reliability index for steel and reinforced concrete buildings located at Chilpancingo, Guerrero (seismic zone D).

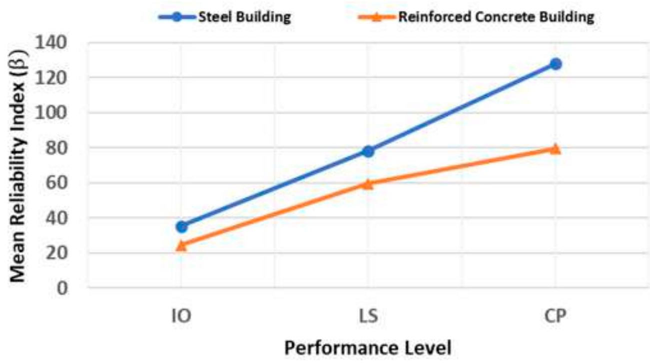

Figure 16. Mean reliability index for steel and reinforced concrete buildings located at Culiacan, Sinaloa (seismic zone B).

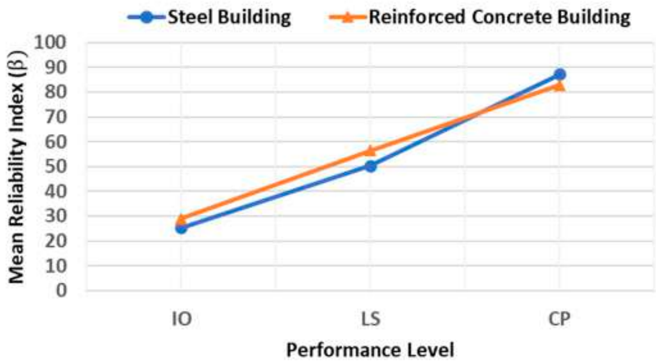

Figure 17. Mean reliability index for steel and reinforced concrete buildings located at Guadalajara, Jalisco (seismic zone C).

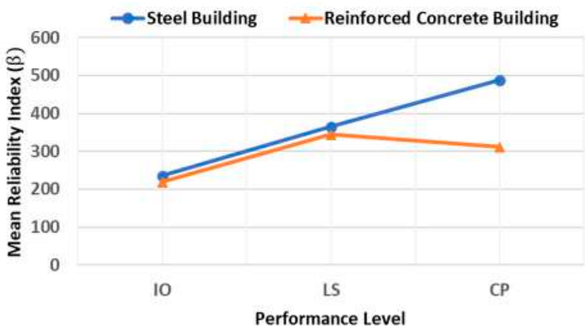

Figure 18. Mean reliability index for steel and reinforced concrete buildings located at Merida, Yucatan (seismic zone A).

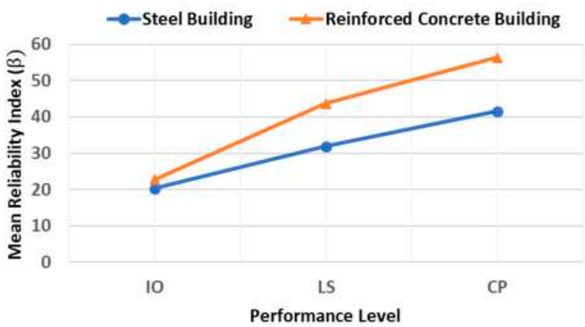

Figure 19. Mean reliability index for steel and reinforced concrete buildings located at Mexicali, Baja California (seismic zone D).

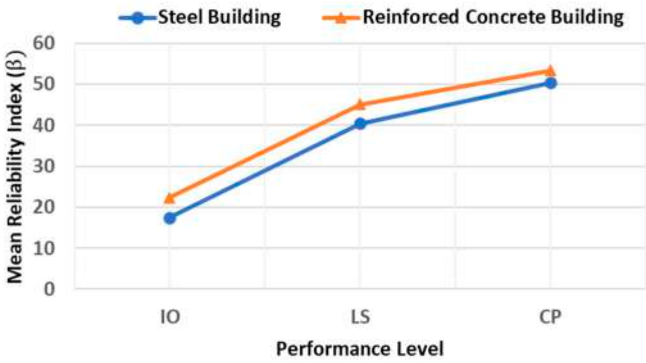

Figure 20. Mean reliability index for steel and reinforced concrete buildings located at Oaxaca de Juarez, Oaxaca (seismic zone D).

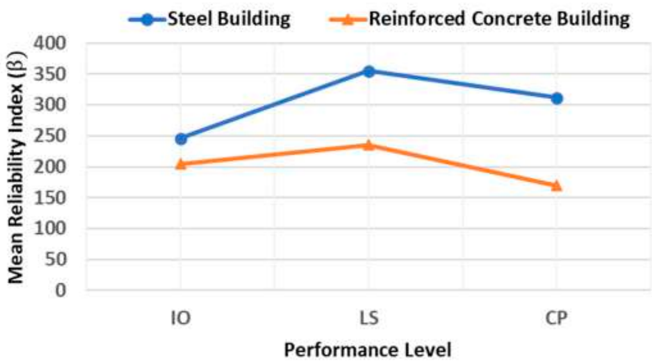

Figure 21. Mean reliability index for steel and reinforced concrete buildings located at Torreon, Coahuila (seismic zone A).

Based on the results presented in Figures 12–21, several observations can be documented. First, it can be observed that the β values for IO, LS, and CP are superior for reinforced concrete structures located in seismic zone D. On the other hand, in most of the cases, steel structures present the highest values of β for IO, LS, and CP for the seismic zones A, B, and C. Based on these observations, reinforced concrete structures have a better performance than steel buildings for earthquake-prone areas in Mexico (seismic zone D). In contrast, steel buildings are generally more reliable than reinforced concrete structures for locations with a low, medium, and somewhat high seismicity (seismic zones A, B, and C). Both steel and reinforced concrete buildings located in seismic zone A exhibit the highest values of β. This is an expected behavior given the fact that very weak ground motions are expected for this seismic zone, which translates into small inter-story drifts in the buildings in the study. Conversely, buildings found in seismic zone D present the lowest values of β. This is reasonable given the ground motions selected for seismic zone D, which are very strong earthquakes that produce larger inter-story drifts, and a decrease in the values of β as a consequence. An interesting observation from Figures 12–21 is the increase in the values of β from the IO to LS performance level. In this context, for six out of ten cases, β increases from the LS to CP performance level, and four out of ten cases present a drop in the values of β. However, these decreases are not that large for any of the cases. Furthermore, focusing on the seismic prone region of Mexico (seismic zone D) it can be observed that from IO to LS and LS to CP there is always an increase in the values of β. This is relevant because there is a high probability of strong ground motions occurring in this zone and causing very large inter-story drifts in the buildings. In addition to the above statements, it is observed that, for most of the cases, the mean reliability index increases for ground motions with higher return periods. This may be justified because earthquakes related to a return period of 2475 years are the strongest ground motions in this study, and their corresponding performance limits are also the largest. Thus, it is unlikely to exceed the performance limit for earthquakes with a return period of 2475 years, and consequently, its reliability is increasing in many of the cases.

Finally, Table 6 summarizes the best-fit probability density functions (PDFs) corresponding to inter-story drifts exhibited by steel and reinforced concrete buildings, respectively. Table 6 is organized in terms of the locations under consideration and the corresponding three performance levels: IO, LS, and CP. As previously mentioned, the following eleven PDFs are used by the probabilistic approach to extract risk: (1) normal, (2) lognormal, (3) Birnbaun–Saunders, (4) extreme value (EV), (5) gamma, (6) generalized extreme value (GEV), (7) logistic, (8) loglogistic, (9) stable, (10) t location scale (tLS), and (11) Weibull (Vazquez-Ontiveros et al., 2021) [36]. Then, based on a Chi-squared test, the best-fit PDF is selected for every case under consideration. In summary, it is clearly observed in Table 6 that the GEV dominates for almost every case. In this context, only for very few cases do the Stable or tLS control the probabilistic analysis. In general, based on these results, it can be stated that the GEV is a very promising PDF to be used for the representation of the stochastic behavior of inter-story drifts of steel and reinforced concrete buildings subjected to earthquake loading.

Table 6. Probability distribution functions for every building and location.

Location	Steel Buildings			Reinforced Concrete Buildings		
	IO	LS	CP	IO	LS	CP
Agua Prieta, Sonora	GEV	GEV	GEV	GEV	GEV	GEV
Ciudad Victoria, Tamaulipas	GEV	GEV	GEV	GEV	GEV	GEV
Villahermosa, Tabasco	Stable	GEV	GEV	GEV	GEV	GEV
Chilpancingo, Guerrero	Stable	GEV	GEV	GEV	GEV	GEV
Culiacan, Sinaloa	GEV	GEV	GEV	GEV	GEV	GEV
Guadalajara, Jalisco	GEV	GEV	GEV	GEV	GEV	Stable
Merida, Yucatan	tLS	GEV	GEV	GEV	GEV	Stable
Mexicali, Baja California	GEV	GEV	GEV	GEV	Stable	GEV
Oaxaca de Juarez, Oaxaca	Stable	GEV	GEV	GEV	Stable	GEV
Torreon, Coahuila	tLS	GEV	GEV	GEV	GEV	GEV

4. Conclusions

Based on the results documented in this paper, several conclusions can be reported as follows:

- A novel probabilistic approach was implemented to extract the structural risk of steel and reinforced concrete buildings in different locations (seismic zones A, B, C, and D) in Mexico. The mean values of maximum inter-story drift demonstrated that buildings located in earthquake-prone regions in Mexico (seismic zone D) present the largest deformations. This is an anticipated scenario, since it is expected that very strong earthquakes occur in these regions.
- Buildings located in regions with a very low seismic activity in Mexico (seismic zone A) exhibited the smallest inter-story drifts. This is logical given the low magnitude earthquakes commonly occurring in those areas. Thus, seismic loading is never significant in these locations. On the other hand, buildings located in zones with the highest seismic hazard (seismic zone D) in Mexico presented the lowest values of reliability index (β). In contrast, those located in seismic zone A (lowest seismic risk) showed the highest values of reliability index (β). This may reflect the tendency of building codes to protect buildings designed in earthquake-prone areas.

- In general, for almost every case under study, it is observed that the structural reliability of buildings increased from IO to LS and LS to CP, respectively, which can reflect a higher structural safety for buildings subjected to very intense ground motions.
- It was demonstrated that the main PDF controlling the stochastic behavior of inter-story drift is the GEV distribution. This is an important observation that implies that the randomness of damage in buildings can be studied using this PDF in the future.

Finally, it must be stated that the above listed conclusions are based only on the results presented in this technical paper. Therefore, it is recommended to perform further analyses to complement what is presented in this manuscript. For example, three-dimensional response history analyses are recommended as well as the consideration of some other locations in Mexico. In addition, comparisons using other probabilistic methods implementing fragility curves are recommended. However, this goes beyond the scope of this paper, and we plan to address these limitations in future publications. We conclude that the principal advantage of the proposed probabilistic approach is that the structural safety in terms of the reliability index (β) can be efficiently extracted by evaluating the most suitable PDF of inter-story drift, which represents the most adequate stochastic behavior of the random variable under consideration. Thus, with the help of the probabilistic approach presented in this paper, it is possible to predict the performance of buildings with a computed level of confidence under different levels of earthquake excitation. This is very important since the accuracy of the seismic response of the buildings, which is used for the risk calculation, will be guaranteed.

Author Contributions: Conceptualization, J.G.M.-Q.; Data curation, F.V.-B. and A.R.-S.; Investigation, A.R.-S. and X.G.T.-C.; Methodology, J.G.M.-Q. and J.R.G.-C.; Project administration, J.R.G.-C.; Resources, F.V.-B. and J.M.L.-G.; Supervision, J.R.G.-C.; Visualization, F.V.-B. and J.M.L.-G.; Writing—original draft, J.G.M.-Q. and J.R.G.-C.; Writing—review and editing, A.R.-S. All authors have read and agreed to the published version of the manuscript.

Funding: The study presented in this paper is supported by two agencies of the government of Mexico: CONACYT and SEP under Grant No. A1-S-10088.

Institutional Review Board Statement: Not applicable.

Informed Consent Statement: Not applicable.

Data Availability Statement: Not applicable.

Acknowledgments: The authors would like to acknowledge the Autonomous University of Sinaloa where all the authors are affiliated. In addition, this work was possible thanks to CONACYT and SEP, which are two very important agencies of the Government of Mexico. Finally, the authors would like to thank the anonymous reviewers of the paper.

Conflicts of Interest: The authors declare no conflict of interest.

References

1. MCBC. Mexico City Building Code. In *Complementary Technical Norms for Earthquake Resistant Design*; Government of Mexico City: Mexico City, Mexico, 2017.
2. IBC. *International Building Code*; International Code Council: Washington, DC, USA, 2012.
3. Esteva, L. The Mexico earthquake of September 19, 1985—Consequences, lessons, and impact on research and practice. *Earthq. Spectra* **1988**, *4*, 413–426. [CrossRef]
4. Kroll, C.A.; Landis, J.D.; Shen, Q.; Stryker, S. Economic impacts of the Loma Prieta earthquake: A focus on small business. *Berk. Plan. J.* **1991**, *5*, 39–58. [CrossRef]
5. Kircher, C.A.; Reitherman, R.K.; Whitman, R.V.; Arnold, C. Estimation of earthquake losses to buildings. *Earthq. Spectra* **1997**, *13*, 703–720. [CrossRef]
6. Olshansky, R.B.; Johnson, L.A.; Topping, K.C. Rebuilding communities following disaster: Lessons from Kobe and Los Angeles. *Built Environ.* **2006**, *32*, 354–374. Available online: https://www.jstor.org/stable/23289510 (accessed on 10 September 2022). [CrossRef]
7. SEAOC Vision 2000. *Performance Based Seismic Engineering of Buildings*; Structural Engineers Association of California (SEAOC): Los Angeles, CA, USA, 1995.
8. *ATC-40*; Seismic Evaluation and Retrofit of Concrete Buildings. Applied Technology Council (ATC): Los Angeles, CA, USA, 1996.

9. *FEMA-273*; NEHRP Guidelines for the Seismic Rehabilitation of Buildings. Federal Emergency Management Agency (FEMA): Los Angeles, CA, USA, 1997.
10. *FEMA-350*; Recommended Seismic Design Criteria for New Steel Moment-Frame Buildings. Federal Emergency Management Agency (FEMA): Los Angeles, CA, USA, 2000.
11. Haukaas, T.; Der Kiureghian, A. Parameter sensitivity and importance measures in nonlinear finite element reliability analysis. *J. Eng. Mech.* **2005**, *131*, 1013–1026. [CrossRef]
12. Der Kiureghian, A.; Haukaas, T.; Fujimura, K. Structural reliability software at the University of California, Berkeley. *Struct. Saf.* **2006**, *28*, 44–67. [CrossRef]
13. Haukaas, T.; Der Kiureghian, A. Strategies for finding the design point in non-linear finite element reliability analysis. *Probabilistic Eng. Mech.* **2006**, *21*, 133–147. [CrossRef]
14. Koo, H.; Der Kiureghian, A.; Fujimura, K. Design-point excitation for non-linear random vibrations. *Probabilistic Eng. Mech.* **2005**, *20*, 136–147. [CrossRef]
15. Au, S.K.; Beck, J.L. First excursion probabilities for linear systems by very efficient importance sampling. *Probabilistic Eng. Mech.* **2001**, *16*, 193–207. [CrossRef]
16. Ching, J.; Au, S.K.; Beck, J.L. Reliability estimation for dynamical systems subject to stochastic excitation using subset simulation with splitting. *Comput. Methods Appl. Mech. Eng.* **2005**, *194*, 1557–1579. [CrossRef]
17. Au, S.K.; Beck, J.L. A new adaptive importance sampling scheme for reliability calculations. *Struct. Saf.* **1999**, *21*, 135–158. [CrossRef]
18. Hamburger, R.O.; Foutch, D.A.; Cornell, C.A. Translating research to practice: FEMA/SAC performance-based design procedures. *Earthq. Spectra* **2003**, *19*, 255–267. [CrossRef]
19. Cornell, C.A.; Jalayer, F.; Hamburger, R.O.; Foutch, D.A. Probabilistic basis for 2000 SAC federal emergency management agency steel moment frame guidelines. *J. Struct. Eng.* **2002**, *128*, 526–533. [CrossRef]
20. Yun, S.Y.; Hamburger, R.O.; Cornell, C.A.; Foutch, D.A. Seismic performance evaluation for steel moment frames. *J. Struct. Eng.* **2002**, *128*, 534–545. [CrossRef]
21. Wen, Y.K. Reliability and performance-based design. *Struct. Saf.* **2001**, *23*, 407–428. [CrossRef]
22. Liao, W.C.; Goel, S.C. Performance-based seismic design of RC SMF using target drift and yield mechanism as performance criteria. *Adv. Struct. Eng.* **2014**, *17*, 529–542. [CrossRef]
23. Franchin, P.; Petrini, F.; Mollaioli, F. Improved risk-targeted performance-based seismic design of reinforced concrete frame structures. *Earthq. Eng. Struct. Dyn.* **2018**, *47*, 49–67. [CrossRef]
24. Harris, J.; Speicher, M. Assessment of performance-based seismic design methods in ASCE 41 for new steel buildings: Special moment frames. *Earthq. Spectra* **2018**, *34*, 977–999. [CrossRef]
25. *ASCE 41-13*; Seismic Evaluation and Retrofit of Existing Buildings. American Society of Civil Engineers (ASCE): Reston, VA, USA, 2014.
26. *ASCE 7-16*; Minimum Design Loads for Buildings and Other Structures. American Society of Civil Engineers (ASCE): Reston, VA, USA, 2016.
27. Gaxiola-Camacho, J.R.; Azizsoltani, H.; Villegas-Mercado, F.J.; Haldar, A. A novel reliability technique for implementation of performance-based seismic design of structures. *Eng. Struct.* **2017**, *142*, 137–147. [CrossRef]
28. Gaxiola-Camacho, J.R.; Haldar, A.; Azizsoltani, H.; Valenzuela-Beltran, F.; Reyes-Salazar, A. Performance-based seismic design of steel buildings using rigidities of connections. *ASCE ASME J. Risk Uncertain. Eng. Syst. Part A Civ. Eng.* **2018**, *4*, 04017036. [CrossRef]
29. Gaxiola-Camacho, J.R.; Haldar, A.; Reyes-Salazar, A.; Valenzuela-Beltran, F.; Vazquez-Becerra, G.E.; Vazquez-Hernandez, A.O. Alternative reliability-based methodology for evaluation of structures excited by earthquakes. *Earthq. Struct.* **2018**, *14*, 361–377. [CrossRef]
30. Moghaddam, H.; Hajirasouliha, I.; Gelekolai, S.M.H. Performance-based seismic design of moment resisting steel frames: Adaptive optimisation framework and optimum design load pattern. *Structures* **2021**, *33*, 1690–1704. [CrossRef]
31. Monjardin-Quevedo, J.G.; Reyes-Salazar, A.; Tolentino, D.; Gaxiola-Camacho, O.D.; Vazquez-Becerra, G.E.; Gaxiola-Camacho, J.R. Seismic reliability of steel SMFs with deep columns based on PBSD philosophy. *Structures* **2022**, *42*, 1–15. [CrossRef]
32. Demir, A. Investigation of the effect of real ground motion record number on seismic response of regular and vertically irregular RC frames. In *Structures*; Elsevier: Amsterdam, The Netherlands, 2022; Volume 39, pp. 1074–1091. [CrossRef]
33. Mazzoni, S.; McKenna, F.; Scott, M.H.; Fenves, G.L. The Open System for Earthquake Engineering Simulation (OpenSEES) User Command-Language Manual. 2006. Available online: https://citeseerx.ist.psu.edu/viewdoc/summary?doi=10.1.1.476.1843 (accessed on 10 September 2022).
34. Demir, A.; Palanci, M.; Kayhan, A.H. Probabilistic assessment for spectrally matched real ground motion records on distinct soil profiles by simulation of SDOF systems. *Earthq. Struct.* **2021**, *21*, 395–411. [CrossRef]
35. Nowak, A.S.; Collins, K.R. *Reliability of Structures*; CRC Press: Boca Raton, FL, USA, 2012.
36. Vazquez-Ontiveros, J.R.; Vazquez-Becerra, G.E.; Quintana, J.A.; Carrion, F.J.; Guzman-Acevedo, G.M.; Gaxiola-Camacho, J.R. Implementation of PPP-GNSS measurement technology in the probabilistic SHM of bridge structures. *Measurement* **2021**, *173*, 108677. [CrossRef]
37. Lemaire, M. *Structural Reliability*; Wiley-ISTE: New York, NY, USA, 2009.